Figure 2. The specific heat of $Cs_2FeCl_5 \cdot H_2O$. The smooth curve represents the fit of the magnetic and lattice contributions; the dashed curve represents the lattice contribution alone.

spin systems as normalized for a spin of $5/2$,[10] with $g = 2.0$. The fitted exchange parameter is -0.65 ± 0.05 K, and a molecular field correction to account for interchain interactions takes the value $zJ'/k = -0.46 \mp 0.05$ K. Several equally good fits can be obtained by varying J/k in one direction and then compensating by a change in the value of zJ'/k. These values combine to yield an average value of $2J/k + zJ'/k \simeq -1.76$ K, which may be compared to the value -1.97 K obtained in the following fashion. The relationship $\chi_\perp(0) = Ng^2\mu_B^2/4|zJ|$ is obtained from both molecular field and spin-wave theories,[8,11] where $\chi_\perp(0)$ is the perpendicular susceptibility in the ordered state, extrapolated to 0 K. For $Cs_2FeCl_5 \cdot H_2O$, our data along the b and c axes suggest $\chi_\perp(0) = 0.19$ emu/mol, which leads to the value of zJ/k given above. Zero-point spin deviations[8] should decrease the experimental value of $\chi_\perp(0)$ by some 5% for $S = 5/2$, causing the exchange constant evaluated in this way to be too large. As with $MnCl_2 \cdot 2H_2O$,[12] intrachain and interchain exchange are of comparable magnitude, causing the usual broad maximum anticipated in the susceptibilities of a chain magnet to be obscured.

On the other hand, a sharp λ peak at 6.57 ± 0.05 K is observed (Figure 2) in the specific heat of $Cs_2FeCl_5 \cdot H_2O$, but none of the usual features expected[7,8] for linear chain magnets are apparent. The measured critical temperatures agree within experimental error. The lattice heat capacity has been evaluated tentatively by an empirical procedure.[1] The magnetic contribution to the heat capacity was evaluated by difference, and allowed an estimate of the magnetic entropy. A value of $\Delta S = R \ln (2S + 1) = 3.56$ cal/mol·K is calculated for iron-(III) systems, and $\Delta S = 3.65$ cal/mol·K was determined in the case of $Cs_2FeCl_5 \cdot H_2O$. One is forced to conclude that the assignment of one-dimensional character from the susceptibility results is more extreme than the true situation.

The parameters describing the other members of the series are included in Table I. The high transition temperatures cause considerable difficulty in an analysis in terms of magnetic model systems, and the other exchange parameters provided must be considered only as suggestive at this time. With the possible exception of the ferromagnetic $A_2CuX_4 \cdot 2H_2O$ series,[8] this set of iron compounds (along with the ammonium and potassium analogues[13]) appears to be the largest series of isostructural ordered magnets currently known. A careful analysis of the heat capacity results is in progress, and the degree of anisotropy present can be best derived from the magnetic phase diagram. It is of interest to note that, for a given alkali ion, T_c for a bromide compound is always higher than that of the chloride analogue. While that is behavior characteristic of many such isomorphous pairs of hydrated

halides,[14] what is novel in these results is the discovery of the T_c dependence upon the alkali ion, A. Since superexchange interactions are known to have approximately an r^{-12} dependence between metal ion centers,[15] a complete crystal structure analysis of each member of this series is required before a rationale can be provided for this result.

References and Notes

(1) Further details may be found in the Ph.D. Thesis of C. J. O'Connor, University of Illinois at Chicago Circle, Aug 1976.
(2) H. P. Klug, D. Kummer, and L. Alexander, *J. Am. Chem. Soc.*, **70**, 3064 (1948).
(3) I. Lindqvist, *Ark. Kemi, Minerol. Geol.*, **24A**, 1 (1946).
(4) J. P. Wignacourt, G. Mairesse, and P. Barbier, *Cryst. Struct. Commun.*, **5**, 293 (1976).
(5) G. M. Cole, Jr., and B. B. Garrett, *Inorg. Chem.*, **13**, 2680 (1974).
(6) T. E. Hopkins, A. Zalkin, D. H. Templeton, and M. G. Adamson, *Inorg. Chem.*, **5**, 1431 (1966).
(7) R. L. Carlin, *Acc. Chem. Res.*, **9**, 67 (1976).
(8) L. J. de Jongh and A. R. Miedema, *Adv. Phys.*, **23**, 1 (1974).
(9) See, for example, L. J. de Jongh, W. D. van Amstel, and A. R. Miedema, *Physica (Utrecht)*, **58**, 277 (1972), for a discussion of this point.
(10) T. Smith and S. A. Friedberg, *Phys. Rev.*, **176**, 660 (1968).
(11) C. Domb and A. R. Miedema, *Prog. Low Temp. Phys.*, **4**, 296 (1964).
(12) J. N. McElearney, S. Merchant, and R. L. Carlin, *Inorg. Chem.*, **12**, 906 (1973).
(13) J. N. McElearney and S. Merchant, unpublished work. These authors find T_c of 6.87 and 7.25 K for $(NH_4)_2FeCl_5 \cdot H_2O$ and 14.06 K for the potassium analogue.
(14) For example, T_c ($NiCl_2 \cdot 6H_2O$) is 5.34 K (W. K. Robinson and S. A. Friedberg, *Phys. Rev.*, **117**, 402 (1960)) while T_c ($NiBr_2 \cdot 6H_2O$) is 8.30 K (S. N. Bhatia and R. L. Carlin, *Physica (Utrecht)*, Ser. B, **86–88**, 903 (1977)). In the case of chained compounds, T_c ($CsMnCl_3 \cdot 2H_2O$) is 4.89 K (R. D. Spence, W. J. M. de Jonge, and K. V. S. Rama Rao, *J. Chem. Phys.*, **51**, 4694 (1969)) while T_c ($CsMnBr_3 \cdot 2H_2O$) is 5.75 K (C. H. W. Swüste, W. J. M. de Jonge, and J. A. G. W. van Meijel, *Physica (Utrecht)*, **76**, 21 (1974)), but on the other hand T_c ([$(CH_3)_3NH$]$CoCl_3 \cdot 2H_2O$]) is 4.14 K (D. B. Losee, J. N. McElearney, G. E. Shankle, R. L. Carlin, P. J. Cresswell, and W. T. Robinson, *Phys. Rev. B*, **8**, 2185 (1973)) while T_c of the analogous bromide is 3.85 K (J. N. McElearney, unpublished work).
(15) L. J. de Jongh and R. Block, *Physica (Utrecht)*, Ser. B, **79**, 568 (1975).
(16) Tata Institute for Fundamental Research, Bombay, India.
(17) Department of Chemistry, University of Virginia, Charlottesville, Va. 22901.

R. L. Carlin,* S. N. Bhatia,[16] C. J. O'Connor[17]

Department of Chemistry
University of Illinois at Chicago Circle
Chicago, Illinois 60680
Received July 14, 1977

Photoelectrosynthesis of Ethane from Acetate Ion at an n-Type TiO$_2$ Electrode. The Photo-Kolbe Reaction

Sir:

Most of the recent interest in semiconductor electrodes has been concerned with their application to photovoltaic cells and to the photoelectrolysis of water to hydrogen and oxygen.[1] Although some studies of the electrochemical behavior of organic substances at semiconductor electrodes have been reported,[2,3] little attention has been paid to photoassisted synthesis at semiconductor electrodes (photoelectrosynthesis). We thought it of interest to extend these studies to a classical electrochemical synthetic reaction, the oxidation of carboxylates (the Kolbe reaction),[4] and report here the photoassisted oxidation of acetate ion to ethane in acetonitrile (ACN) solutions at n-type TiO_2 electrodes in both the single-crystal and chemically vapor deposited polycrystalline[5] form. This reaction is of interest because it should provide a means of using solar
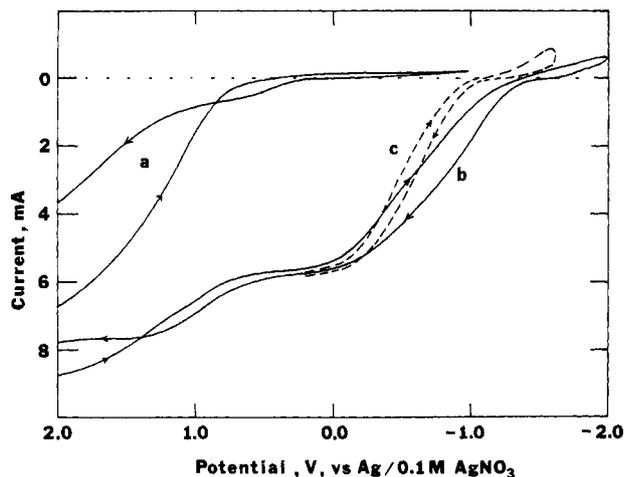
Figure 1. Current–potential curves for single-crystal n-TiO₂ during illumination with a 450-W Xenon lamp: (a) in ACN/0.1 M TBAP (background); (b) in ACN/0.1 M TBAP containing 0.08 M TBAAc; (c) in ACN/0.1 M TBAP containing 0.08 M TBAAc and ~0.1 M acetic acid.

energy to produce hydrocarbons via the widely studied Kolbe reaction.

The reaction typically was carried out in a vacuum-tight one-compartment Pyrex cell which was fitted with a flat window. The cell was equipped with single-crystal n-type TiO_2[6] and platinum disk working electrodes, a platinum (wire or foil) counterelectrode, and a silver wire reference electrode. Acetonitrile[7] containing 0.1 M tetra-n-butylammonium perchlorate (TBAP) was used as the reaction medium to minimize competition due to solvent oxidation.[8] This reaction medium was shown by Russell and Anson[9] to be suitable for a clean Kolbe oxidation of acetate on platinum and to give a high yield of ethane even at low current density. The voltammetric behavior at n-TiO_2 in this medium (Figure 1) clearly shows the photooxidation of acetate. No faradaic current is observed in the dark at a single-crystal n-TiO_2 electrode in a solution containing 0.08 M tetra-n-butylammonium acetate (TBAAc)[10] and 0.1 M TBAP in ACN until potentials above +5 V vs. Ag/0.1 M AgNO₃ in ACN. The oxidation of the background solution, 0.1 M TBAP–ACN, at an illuminated (450-W Xe lamp) n-TiO_2 electrode begins at a potential of about 0 V vs. Ag/0.1 M AgNO₃ with the photocurrent becoming significant beyond ~1 V vs. Ag/0.1 M AgNO₃ (curve a). Upon addition of acetate ion (i.e., 0.08 M TBAAc) a broad anodic wave beginning at −1.6 V vs. Ag/0.1 M AgNO₃ was observed at an illuminated TiO₂ electrode (curve b). The height of this wave showed a pronounced concentration dependence at small acetate concentrations and attained a height of ~65% of the limiting background photocurrent for 0.08 M acetate. Thus the photoassisted oxidation of acetate occurs at potentials ~2.4 V negative of where acetate oxidation occurs on Pt.[11]

To confirm that the products for the photooxidation were the same as those for the electrooxidation at platinum in ACN, bulk electrolysis was carried out. For a typical run ~9 mL of ACN was condensed under reduced pressure into the cell, containing 1.0 g of TBAAc (3.3 mmol), 150 μL of acetic acid (2.5 mmol), and 340 mg of TBAP (1 mmol) to give ~10 mL of a colorless solution. Helium gas was allowed to fill the rest of the cell until a pressure of ~600 mm was reached whereupon the cell was closed tightly. When the face of the single-crystal n-TiO_2 electrode (0.5 cm²) was irradiated (through the window) with the full output of a 450-W Xenon lamp, a broad oxidation wave appeared, showing an onset of anodic photocurrent at ca. −1.0 V vs. Ag-wire reference and a limiting current of ~10 mA at potentials at or above +0.5 V. (The shift

to negative potentials of the onset of photooxidation on n-TiO₂ due to the basic acetate ions is counteracted by acetic acid, curve c.) The preparative electrolysis was performed with the photoanode maintained at 0.0 V vs. Ag, where an initial photocurrent of ~5.5 mA was recorded. Gas bubbles were formed at the illuminated semiconductor anode accompanied by vigorous gas evolution at the platinum-wire cathode. The photocurrent decayed during the first 30 min to ~4 mA; it stayed at about this level throughout the continuous photoelectrolysis of ~9 h, yielding 109 C. The evolved gases, temporarily stored in the upper part of the electrolysis cell, were transferred after the electrolysis into a gas sample tube and analyzed by mass spectrometry.

The low resolution mass spectrum of such a gas mixture showed strong signals of carbon dioxide (m/e 44 (rel intensity, 100%)), acetonitrile (m/e 41 (40%), 40 (20%), 39 (9%), 38 (5%)), and ethane (m/e 30 (14%), 29 (12%), 28 (68%), 27 (16%), 26 (9%)), as well as background signals of O₂ (m/e 32 (10%)), N₂ (m/e 28, which overlaps the main signal of ethane), and H₂O (m/e 18 (80%), 17 (17%)), and other signals at m/e 16 (14%), 15 (12%), 14 (4%). The contamination signals of O₂, N₂, and H₂O were also found in a background spectrum. After correction for the N₂ signal (taken as ~30% relative intensity), the signals of m/e 26–30 fitted well a reference spectrum for ethane.[13] By high resolution mass spectroscopy the peak at m/e 30 was clearly established to be due to the ethane molecule ion, as the ratio m/e was determined to be 30.046 91, compared with a theoretical ratio of 30.046 95 for ethane (thus eliminating the improbable alternative H₂CO). The current efficiency for acetate oxidation was obtained by sweeping the CO₂ produced during electrolysis out of the cell using a stream of nitrogen into an aqueous solution of Ba(OH)₂, causing precipitation of BaCO₃. The amount of CO₂ produced during electrolysis, determined by weighing the precipitate, yielded an overall current efficiency of at least 64% for the photooxidation. The (potential and concentration dependent) quantum efficiency for acetate oxidation for light of energy greater than the band gap energy, E_g, of 3.1 eV, estimated from the limiting background photocurrent and the measured current for acetate oxidation, was ~65% at 0 V vs. Ag/0.1 M AgNO₃ for 0.08 M TBAAc.

The reaction mechanism thus follows that for other photoassisted oxidations at n-TiO_2. Light of energy greater than E_g causes formation of electron-hole pairs. When the potential of the semiconductor is positive of the flat-band potential, the bands are bent upward and the photogenerated holes (p⁺) migrate to the electrode surface while the electrons drift to the bulk of the electrode, thus preventing recombination. The holes, at energies characteristic of the valence band or low lying surface states, are effectively strong oxidizing agents and can abstract electrons from acetate ions initiating the cascade of steps in the Kolbe reaction:

$$CH_3CO_2^- + p^+ \rightarrow CH_3\cdot + CO_2 \qquad (1)$$

$$2CH_3\cdot \rightarrow C_2H_6 \qquad (2)$$
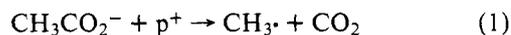
Since the photo-Kolbe reaction occurs at potentials ~2.4 V more negative than those for the oxidation at platinum, the effective efficiency of utilization of the excitation energy is high. The chemical irreversibility of the overall process prevents back-donation of electrons from the electrode and leads to an overall high efficiency for the process.[14] The potential for the photooxidation of acetate is negative of that for the onset of hydrogen ion reduction in the acetate/acetic acid mixture (ca. −0.8 V vs. Ag-wire reference), suggesting that photoelectrolysis with little or no external applied voltage leading to a mixture of ethane and hydrogen is possible.[15] Furthermore the control of current density via the light flux and the possible suppression of undesirable two-electron oxi-

dations by the use of photoinduced electron transfer at a wide band gap semiconductor (e.g., TiO_2) are also of interest with respect to the Kolbe electrosynthesis. These subjects are currently being investigated in this laboratory.[16]

References and Notes

(1) See, e.g., A. Fujishima and K. Honda, *Nature (London)*, **238**, 37 (1972); H. Gerischer, *J. Electroanal. Chem.*, **58**, 263 (1975); M. D. Archer, *J. Appl. Electrochem.*, **5**, 17 (1975), and references therein.

(2) T. Freund and W. P. Gomes, *Catal. Rev.*, **3**, 1 (1969); H. Gerischer and H. Roessler, *Chem.-Ing. Techn.*, **42**, 176 (1970); K. Nakatani and H. Tsubomura, *Bull. Chem. Soc., Jpn.*, **50**, 783 (1977).

(3) S. N. Frank and A. J. Bard, *J. Am. Chem. Soc.*, **99**, 303 (1977); S. N. Frank and A. J. Bard, *ibid.*, **99**, 4667 (1977).

(4) H. Kolbe, *Justus Liebigs Ann. Chem.*, **69**, 257 (1849); C. K. Mann and K. K. Barnes, "Electrochemical Reactions in Nonaqueous Systems", Marcel Dekker, New York, N.Y., 1970, Chapter 4.

(5) K. L. Hardee and A. J. Bard, *J. Electrochem. Soc.*, **122**, 739 (1975).

(6) Single-Crystal TiO_2, *001* surface area $\sim$0.5 cm^2 doped under H_2/600 °C/35 min; polished with 0.5-μ alumina, etched 30 s with concentrated HNO_3, rinsed with distilled H_2O, dried in vacuum for $\sim$1 h; electrical contact via silver epoxy cemented Cu wire on the back, protected by silicone adhesive.

(7) The purification of acetonitrile described in S. N. Frank, A. J. Bard, and A. Ledwith, *J. Electrochem. Soc.*, **122**, 898 (1975).

(8) S. N. Frank and A. J. Bard, *J. Am. Chem. Soc.*, **97**, 7427 (1975); P. A. Kohl and A. J. Bard, *ibid.*, in press.

(9) C. D. Russell and F. C. Anson, *Anal. Chem.*, **33**, 1282 (1961).

(10) Prepared by mixing 50 mL of 1.0 M tetrabutylammonium hydroxide in methanol (Southwestern Analytical Chemicals, Inc.) with 3.1 g of glacial acetic acid (Fisher Scientific Co.) and removal of solvent at 60 °C (vacuum) for 2 h followed by drying for 5 days at room temperature and 10^{-4} Torr.

(11) Cyclic voltammetry at a platinum electrode shows E_{pa} = 1.2 V vs. Ag/0.1 M AgNO$_3$, 0.1 M TBAP, ACN for acetate oxidation (scan rate 0.2 V/s).[12]

(12) D. H. Geske, *J. Electroanal. Chem.*, **1**, 502 (1959/60), reported a half-wave potential of +1.58 to 1.63 V vs. SCE under similar conditions.

(13) Reference data for the mass spectrum (rel intensity) of ethane (from "Selected Mass Spectral Data", API, 1972: m/e 30 (26%), 29 (21%), 28 (100%), 27 (33%), 26 (26%).

(14) Oxygen was not photogenerated in noticeable quantities; small amounts of methane (as reported in ref 9 as a side product of oxidation on Pt) cannot be excluded (signal at m/e 16 showed two spikes).

(15) The gas evolving at the platinum cathode did not show a mass spectrum (range, m/e 12–100). There exists little doubt that the reduction of acetate/acetic acid on the low overvoltage Pt electrode yielded hydrogen gas. The overall process in the cell can therefore be rewritten:

$$2CH_3CO_2H \rightarrow CH_3CH_3 + H_2 + 2CO_2$$

(16) The support of this research by the Schweizerische Nationalfonds zur Foerderung der wissenschaftlichen Forschung (to B.K.) and by the National Science Foundation and the Robert A. Welch Foundation is gratefully acknowledged.

Bernhard Kraeutler, Allen J. Bard*

Department of Chemistry, the University of Texas at Austin
Austin, Texas 78712

Catalytic Activity of Nearly Zero-Coordinated Calcium Ion in Fully Ion-Exchanged Calcium-A Zeolite

Sir:

The unit cell of molecular sieve zeolite A has three eight-membered oxygen rings, eight six-membered ones, and twelve four-membered ones. The exchangeable cations in zeolite A can occupy a site near the center of the 8-ring (named α site), that of the 6-ring (β site), or that of 4-ring (γ site). The site selectivities of various cations have been extensively studied.[1] The γ site has weak affinities for all cations. Calcium ion has a strong affinity only for the β site. However, it was found recently that at least one Ca^{2+} per unit cell occupies the α site in Ca_6-A zeolite, and is nearly zero coordinated.[2,3] This Ca^{2+} is expected to have a high catalytic activity, since it is weakly bonded to the 8-ring oxygen and has an unusual coordination. In the present work, this expectation was verified by using Ca_6-A as a catalyst for the isomerization of but-1-ene to *trans*- and *cis*-but-2-enes. This is the first demonstration of chemical

Table I. Catalytic Activities of (Na,Ca)-A Zeolites for Isomerization Reaction of But-1-ene

Catalyst	Reaction temp, °C	Pressure, Torr	Initial rate of isomn, % min^{-1} g^{-1}
Powder Ca_6-A, No. 1	150	16	3.2
Powder Ca_6-A, No. 2	150	16	3.0
Powder $(Na_{1.8}Ca_{5.1})$-A	150	16	2.4
Powder $(Na_{3.6}Ca_{4.2})$-A	150	17	0.31
Pellet Ca_6-A	150	15	14.5
Pellet $(Na_3Ca_{4.5})$-A	150	15	0.45
Bead Ca_6-A	150	15	3.2
Bead $(Na_3Ca_{4.5})$-A	150	15	0.001
Pellet Ca_6-A	200	15	>50
Pellet $(Na_3Ca_{4.5})$-A	200	13	1.2
Bead Ca_6-A	200	18	10.0
Bead $(Na_3Ca_{4.5})$-A	200	14	0.82

effects of the zero-coordination that Seff et al. have found by structural analyses.[3,4]

Catalysts of powder form with compositions Ca_6-A, $(Na_{1.8}Ca_{5.1})$-A, and $(Na_{3.6}Ca_{4.2})$-A were prepared by a method described in a previous paper.[2] Ca_6-A catalyst in pellet or bead form was obtained by treating commercial 5A zeolite with a nominal composition $(Na_3Ca_{4.5})$-A repeatedly with a solution of 0.2 N $CaCl_2$ at 85 °C.

The isomerization was carried out at 150 °C and 200 °C in a closed recirculation reaction having a volume of $\sim$1570 mL. The catalyst was evacuated at 380 °C for 8 h prior to the reaction, and discarded after a single use to avoid possible trouble due to the polymerization of butene. The reaction mixture was periodically withdrawn from the system and subjected to gas chromatographic analysis, in which a 6-m column packed with propylene carbonate on Uniport C (Gas-Chro Industry Co.) was operated at 0 °C. But-1-ene was obtained from Takachiho Chemical Co. and purified by passage through zeolite at -78 °C.

Curves for amounts of isomers of butene vs. reaction time are well described by first-order kinetics. Let us represent the activity of a catalyst by the initial slope of such a curve for but-1-ene. Catalytic activities of various samples are tabulated in Table I. This table shows that the Ca_6-A form was always the most active, whatever form the catalyst was in, be it powder, pellet, or bead, and at whatever temperature, 150 or 200 °C.

The concentration of Ca^{2+} on the α site per unit cell, [Ca/α], has been determined to be 1.3 for the present powder-form Ca_6-A.[2] If it is assumed that [Ca/α] in $(Na_{12-2x}Ca_x)$-A is the same as that in $(K_{12-2x}Ca_x)$-A, it is 0.4 and 0.0 for $(Na_{1.8}Ca_{5.1})$-A and $(Na_{3.6}Ca_{4.2})$-A, respectively.[2] This assumption may be justified by the following consideration. Ca^{2+} prefers the β site over other sites, and the α site is an uncomfortable residence for it. All β sites crowd on the surface of the sodalite unit which can be considered the unit block constituting the framework of zeolite A. Hence, only a limited number of Ca^{2+} can reside at β sites, since the uneven charge distribution increases the electrostatic energy of the crystal. In (K,Ca)-A, for instance, its population limit is 4 ions per unit cell.[2] The same limit may exist with (Na,Ca)-A, because the electrostatic energy plays the leading role in limiting the population.

In the above catalysts, the activity increases with increasing [Ca/α], though not linearly. It is considered that the reaction was partially retarded by the slow diffusion of the reaction products through the small zeolitic pores, and hence that the catalytic activity did not increase linearly with the concentration of active centers. This view is supported by a low activation energy ($\sim$9 kcal/mol) for pellet 5A and bead Ca_6-A samples.